Stanford Exploration Project, Report 79, November 16, 1997, pages 1–135

Stanford Exploration Project, Report 79, November 16, 1997, pages 1–135

Prestack phase-shift migration for separate offsets

Alexander M. Popovici[1]

keywords: *algorithm, phase, Fourier transform, sampling, prestack, velocity*

ABSTRACT

The straightforward implementation of the double square root (DSR) equation in common midpoint and offset coordinates for prestack migration produces notable artifacts that are routinely attributed to Fourier domain wraparound in the offset wavenumber space. These artifacts usually preclude the use of DSR for separate constant-offset sections. I show that the artifacts are not due to Fourier wraparound. I present two phase-shift constant-offset migration algorithms free of offset artifacts. The first algorithm migrates each individual constant-offset at a time, but is slower overall than the second algorithm which requires all the constant-offset sections to be migrated at the same time. Depending on the problem to be solved one method could be more convenient than the other.

INTRODUCTION

Working on migration to zero-offset (MZO) in variable velocity media, I encountered a problem with the formulation of my MZO operator: while the operator is accurate in depth variable velocity, it is defined in the offset-wavenumber domain, and therefore has to be applied to all the offsets at the same time. As people apply DMO to constant-offset sections, I had to look at how to separate the operator so it could be applied to individual offsets. My MZO formulation (Popovici, 1993) is very similar to prestack migration in Fourier domain which also applies a phase-shift operator in offset-wavenumber domain. Therefore I decided to apply the offset separation technique to prestack Fourier domain migration as it is a well known operator and researchers are more familiar with its formulation.

I present two methods for applying phase-shift migration to separate constant-offset sections. One method is faster when applied to all the offsets at the same time. However, this method migrates all the constant-offsets at the same time, so it is inefficient when a single constant-offset migrated image is desired. The second method migrates one constant-offset at a time, but requires more time to migrate all the offsets.

[1]**email:** not available

I also discuss the source of artifacts present in offset domain and explain how they can be avoided by a careful implementation of the algorithm.

DSR equation

Constant velocity **prestack migration** in offset-midpoint coordinates (Yilmaz, 1979) can be formulated as:

$$p(t=0,k_y,h=0,z) = \int d\omega \int dk_h \; e^{ik_z(\omega,k_y,k_h)z} p(\omega,k_y,k_h,z=0), \tag{1}$$

where $p(\omega,k_y,k_h,z=0)$ is the 3-D Fourier transform of the field $p(t,y,h,z=0)$ recorded at the surface, using Claerbout's (1985) sign convention:

$$p(\omega,k_y,k_h,z=0) = \int dt \; e^{i\omega t} \int dy e^{-ik_y y} \int dh e^{-ik_h h} p(t,y,h,z=0).$$

The phase $k_z(\omega,k_y,k_h)$ is defined in the dispersion relation as

$$k_z(\omega,k_y,k_h) \equiv -\text{sign}(\omega) \left\{ \left[\frac{\omega^2}{v^2} - \frac{1}{4}(k_y+k_h)^2 \right]^{\frac{1}{2}} + \left[\frac{\omega^2}{v^2} - \frac{1}{4}(k_y-k_h)^2 \right]^{\frac{1}{2}} \right\}, \tag{2}$$

which is also referred to as the double square-root (DSR) equation. The two integrals in ω and k_h in equation (1) represent the imaging condition for zero-offset and zero time ($h=0, t=0$).

In equation (1), the values of k_z have to be real. Imaginary values of k_z do not satisfy the downward continuation ordinary differential equation

$$\frac{\partial^2 P}{\partial z^2} = -k_z^2 P \tag{3}$$

and have to be excluded. Real values of k_z in equation (2) require both of the following conditions to be satisfied:

$$\begin{cases} \frac{2}{v} \mid \omega \mid & \geq & \mid k_y + k_h \mid \\ \frac{2}{v} \mid \omega \mid & \geq & \mid k_y - k_h \mid . \end{cases}$$

By considering the four possible sign cases, given by assigning k_y and k_h positive and negative values, these two conditions can be reduced to the condition:

$$\frac{2}{v} \mid \omega \mid \;\; \geq \;\; \mid k_y \mid + \mid k_h \mid . \tag{4}$$

Equation (4) will prove to be crucial in determining the source of artifacts that appear in constant-offset migrated sections (Figure **??**a).

The prestack DSR algorithm using constant sampling in k_h can be summarized as:

FFT along all axes $p(t,y,h) \rightarrow P(\omega,k_y,k_h)$
do z
  do k_y
  do ω
  do k_h
  if($\frac{2}{v}$abs(ω) > abs(k_y) + abs(k_h)) then
    $P(\omega,k_y,k_h) = P(\omega,k_y,k_h)e^{ik_z dz}$
    $M(z,k_y) = M(z,k_y) + P(\omega,k_y,k_h)$
  endif

Note that in order to perform an FFT along the offset axis, the variable k_h is evenly sampled between the Nyquist negative and positive values. However, due to condition (4), for each set of ω, k_y the loop in k_h will use either a subset or all of the possible k_h sampled values.

OFFSET SEPARATION

The DSR migration can be put in a form to allow for separate migration of each constant-offset section. However, the overall cost of migrating all the constant-offset sections can be reduced if the processing is done to the whole prestack data cube at the same time. In the next sections I present variations on the DSR migration algorithm that can be used to obtain prestack images for individual offsets. The DSR migration for a single constant-offset section can be used when a particular section needs to be processed. When all the prestack data needs to be processed, the second algorithm is faster.

Migration for a single constant-offset section

Consider a single 2-D constant-offset section $p(t,y;h_0)$ corresponding to a half-offset h_0 in a 3-D cube where all the other constant-offset sections are zero. This is equivalent to introducing a Dirac δ function in offset coordinates. The Fourier transform over offset of such a 3-D field is

$$P(\omega,k_y,k_h) = e^{-ik_h h_0} p(\omega,k_y;h_0).$$

Substituting this wavefield in equation (1), the prestack migration equation can be written as

$$\begin{aligned} p(t=0,k_y,h=0,z) &= \int d\omega \int dk_h \; e^{ik_z(\omega,k_y,k_h)z} e^{-ik_h h_0} p(\omega,k_y;h_0) \\ &= \int d\omega \; p(\omega,k_y;h_0) \int dk_h \; e^{ik_z(\omega,k_y,k_h)z - ik_h h_0}. \end{aligned} \tag{5}$$

The DSR algorithm can be rewritten, extracting the multiplication with the wavefield $P(\omega, k_y; h_0)$ outside the k_h loop.

FFT along t, y axes $p(t, y; h_0) \rightarrow P(\omega, k_y)$
forall k_y, ω, k_h; $ph(\omega, k_y, k_h) = e^{-ik_h h_0}$
do z
  do k_y
  do ω
    do k_h
    $ph(\omega, k_y, k_h) = ph(\omega, k_y, k_h) e^{ik_z dz}$
    $phase(\omega, k_y) = phase(\omega, k_y) + ph(\omega, k_y, k_h)$
  $M(z, k_y) = M(z, k_y) + P(\omega, k_y) * phase(\omega, k_y)$

The loop in k_h becomes a mere numerical integration of the exponential term, integral which can asymptotically approximated through the use of the stationary phase (Appendix A). For depth variable velocity, we have to sum the phase terms corresponding to each depth level. In other words, for depth variable velocity the exponential term contains the sum of all the phases corresponding to previous depth levels. Just knowing the stationary phase for a depth level is not enough to carry the computation to the next depth level.

This is a terribly slow prestack phase-shift migration algorithm that migrates one constant-offset section in almost the time necessary to migrate all constant-offset sections. The algorithm can be sped up hundreds of times if a good stationary phase approximation can be found to the integral

$$\int dk_h e^{ik_z z - ik_h h_0}. \tag{6}$$

Such an algorithm would become:

FFT along t, y axes $p(t, y; h_0) \rightarrow P(\omega, k_y)$
do z
  do k_y
  do ω
  compute *phase* fast
  $M(z, k_y) = M(z, k_y) + P(\omega, k_y) * phase$

In Appendix A, I discuss different properties of the phase function and how the stationary phase could be computed numerically. I could not find an analytical solution for the stationary phase, as it involves finding the roots of a polynomial of sixth degree. However, even if an analytical solution is found for constant velocity, for depth variable velocity the solution incorporates the sum of phases corresponding to different depth slices.

Migration for all constant-offset sections

Another way to greatly improve the speed of the algorithm is to process all the constant-offset sections at the same time. In this case the phase loop can be computed once for all the offsets. The need to keep the constant-offset sections separated is accomplished by observing that the DSR equation can be rewritten in an offset separable form

$$\begin{aligned} p(t=0,k_y,h=0,z) &= \int d\omega \int dk_h \; e^{ik_z(\omega,k_y,k_h)z} \int dh \; e^{-ik_h h} p(\omega,k_y,h) \\ &= \int dh \int d\omega \; p(\omega,k_y,h) \int dk_h \; e^{ik_z(\omega,k_y,k_h)z - ik_h h}. \end{aligned} \tag{7}$$

The integral in h stacks the independently prestack migrated constant-offset sections. As we are interested in each constant-offset section, we rewrite the DSR in an offset separable form

$$p(t=0,k_y,h,z) = \int d\omega \; p(\omega,k_y,h) \int dk_h \; e^{ik_z(\omega,k_y,k_h)z - ik_h h} \tag{8}$$

and observe that the integral in k_h can be replaced by a fast Fourier transform of the exponential

$$e^{ik_z(\omega,k_y,k_h)z}.$$

The algorithm becomes:

FFT along t, y axes $p(t, y; h_0) \rightarrow P(\omega, k_y)$
do z
  do k_y
  do ω
    do k_h
    $ph(\omega, k_y, k_h) = ph(\omega, k_y, k_h) e^{ik_z dz}$
    $phase(\omega, k_y, k_h) = ph(\omega, k_y, k_h)$
  FFT $phase$ along k_h axis
  $M(z, k_y, h) = M(z, k_y, h) + P(\omega, k_y, h) * phase(\omega, k_y, h)$

This algorithm can be executed in parallel for all the values of ω, k_y. Note that for depth variable velocity the phase is carried from one depth level to another, corresponding to an integral in depth of the phase terms corresponding to each depth slice.

DSR artifacts

A straightforward implementation of the DSR equation produces significant artifacts. Several researchers pointed out these artifacts as an inhibiting factor in using the DSR for separate constant-offset sections. A commonly used argument is that the artifacts are due to Fourier domain wraparound along the offset axis. Figure **??**a shows the output of the DSR migration applied to a data cube (t, y, h) containing a single spike in a constant-offset section with an half-offset $h_0 = 190m$. The shallower ellipse is an artifact. Compare this with the output of the improved DSR migration in Figure **??**b. Because of the stacking in offset that is implicitly done in the DSR equation, the artifacts are attenuated. However, when each constant-offset section is taken separately, the artifacts are a disturbing presence.

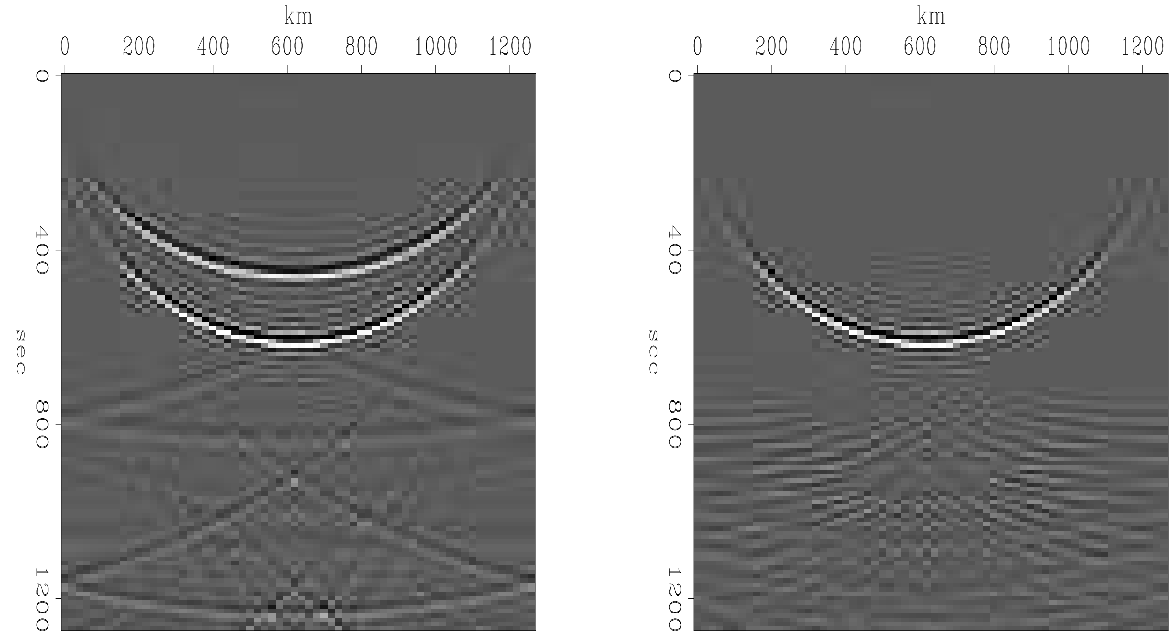

a. Classic DSR migration b. DSR without offset artifacts

Figure 1: The output of DSR in offset-midpoint migration. The input cube contains a single spike for the constant-offset section $h = 190m$.
a. Classic DSR migration. The shallower ellipse is an artifact.
b. DSR migration without offset artifacts. $\boxed{\text{mihai-Fig1}}$ [CR]

The source of artifacts is equation (4), which limits the interval of existence for the variable k_h. Normally the offset-wavenumber k_h is evenly sampled between the values $(-\frac{\pi}{dh}, \frac{\pi}{dh})$ in the DSR offset-midpoint equation, necessary for the FFT along the offset axis. However, the requirement for the square-root expressions to be real limits the available values for k_h. Let's examine equation (4) again:

$$\frac{2}{v} \mid \omega \mid - \mid k_y \mid \geq \mid k_h \mid .$$

When only a subset of the values of k_h are used from the whole set of discrete values, artifacts are introduced in the phase expression. Consider the form of the DSR equation presented in equation (8):

$$p(t=0,k_y,h,z) = \int d\omega\; p(\omega,k_y,h) \int dk_h\; e^{ik_z(\omega,k_y,k_h)z - ik_h h},$$

where the integral in k_h has the integration limits

$$k_h \in \left(-\frac{2}{v} \mid \omega \mid + \mid k_y \mid, \frac{2}{v} \mid \omega \mid - \mid k_y \mid\right), \tag{9}$$

the region of integration can be much smaller than the domain in which k_h is sampled. As a result only several discrete values of k_h are used to evaluate the integral. The missing offset-wavenumbers introduce artifacts, as the interval of existence of the phase is not sufficiently sampled. The correct implementation should subsample the k_h variable between the integration limits and not between some predetermined limits.

Equation (9) is used to migrate a single impulse in a constant-offset section with $h = 190m$, using constant sampling in k_h for all the values ω, k_y. In Figure **??** the only difference between the two migration programs is the offset spacing. Bigger sampling in offset implies smaller sampling in offset-wavenumber. As a result more offset-wavenumber samples are used to compute the phase and reduce the artifacts. The ideal algorithm will use all the available samples, dividing the integration limits in equation (9) by the total number of offsets (assumed to be equal to the number of offset-wavenumbers). This will not preclude the use of FFT to transform the phase from offset-wavenumber domain to offset domain, because for each pair of values ω, k_y, the variable k_h is evenly sampled in the domain of definition.

In order to use the different results of DSR migration algorithms I create a prestack model consisting of 64 constant-offset sections over three vertical diffractors in a depth variable velocity medium. The velocity model is shown in Figure **??**a while an example of the zero-offset travel-time map is shown in Figure **??**b. Figure **??**a shows a zero-offset common midpoint (CMP) section, while Figure **??**b shows the CMP section corresponding to the longest offset ($h = 630m$).

The prestack model was migrated using several variations of the DSR migration algorithm. Figures **??**a and **??**b compare the results of DSR migration via the classic algorithm implementing equation (1) and the results of DSR migration for separate offsets implementing equation (8) using a FFT to transform the phase. In both cases k_h was constantly sampled. To obtain Figure **??**b all the separate constant-offset sections were stacked in the end. The two results are identical as is expected.

Figure **??**a represents the results of DSR migration by implementing equation (8) directly. The integral in k_h is calculated numerically for each offset. The algorithm is slower than the one evaluating the integral in k_h via FFT, but it does not require the migration of all the separate constant-offset sections at the same time. Figure **??**b represents the results of DSR migration with different sampling in k_h for each

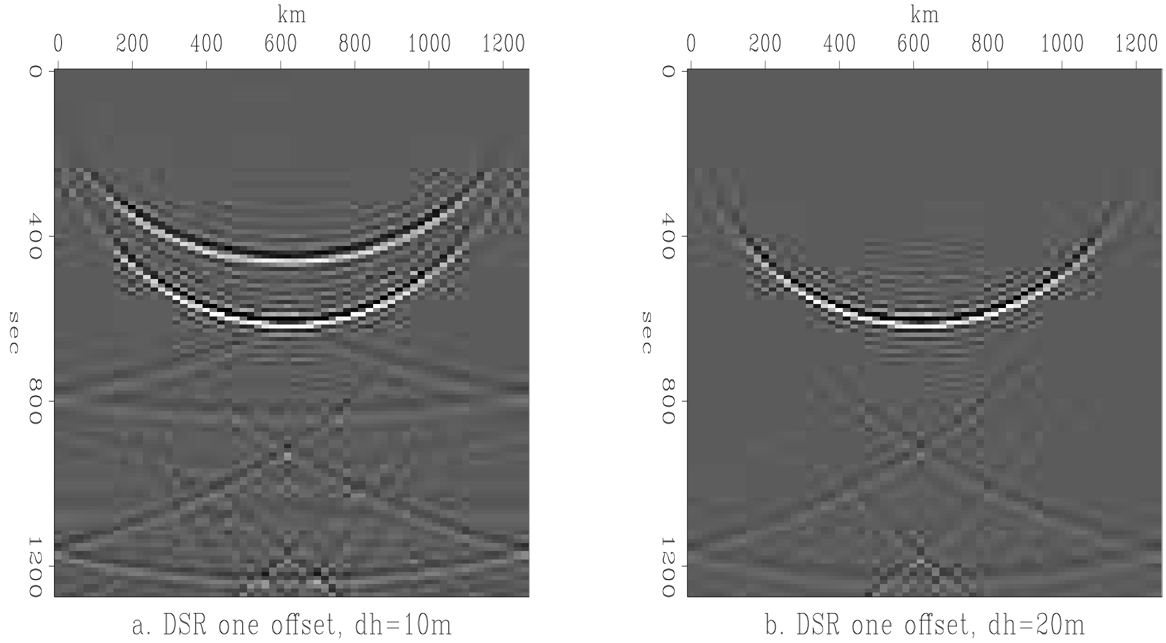

Figure 2: Migration of a single constant-offset section using the separable DSR equation. In the two sections I use the same parameters, excepting the k_h spacing. In the right figure dk_h is smaller.
a. Constant-offset phase-shift migration, $h = 10m$.
b. Constant-offset phase-shift migration, $h = 20m$. mihai-Fig2 [CR]

(ω, k_y) pair. Because stacking attenuates the artifacts the difference between the two algorithms is not as visible in the migrated CMP section.

Figure **??** compares the migrated results of the same CMP, for different offsets. The figure was obtained by slicing vertically the migrated data set. The slice passes through the location of the three diffraction events shown in Figure **??**. A correctly migrated image should show the same events for all the offsets. Figure **??**a displays the diagonal artifacts that appear using constant k_h sampling. The diagonal stripes create the ghost ellipse in Figure **??**a. Figure **??**b is obtained using separate sampling of k_h for each (ω, k_y) pair, and all artifacts are virtually eliminated.

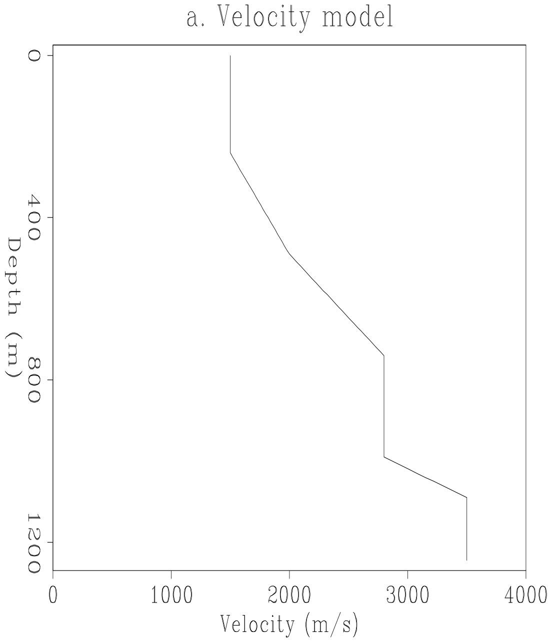

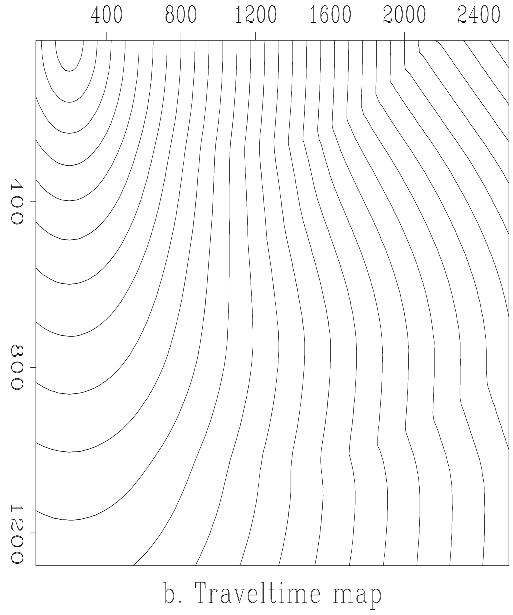

Figure 3: Depth variable velocity model.
a. Interval velocity used.
b. Zero-offset traveltime map used for modeling. mihai-Fig3 [CR]

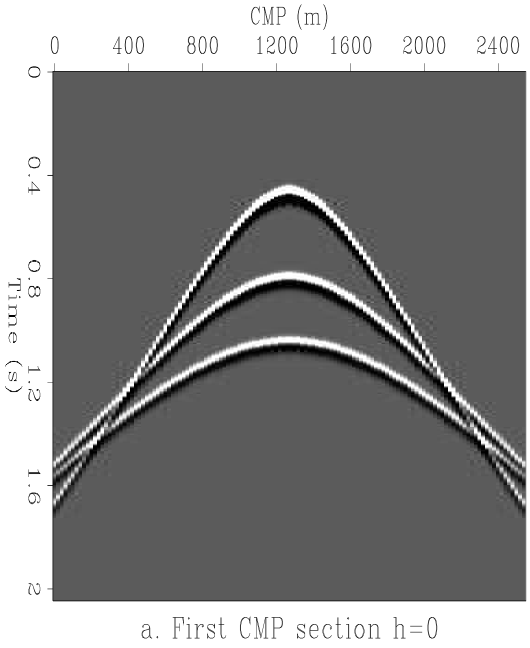

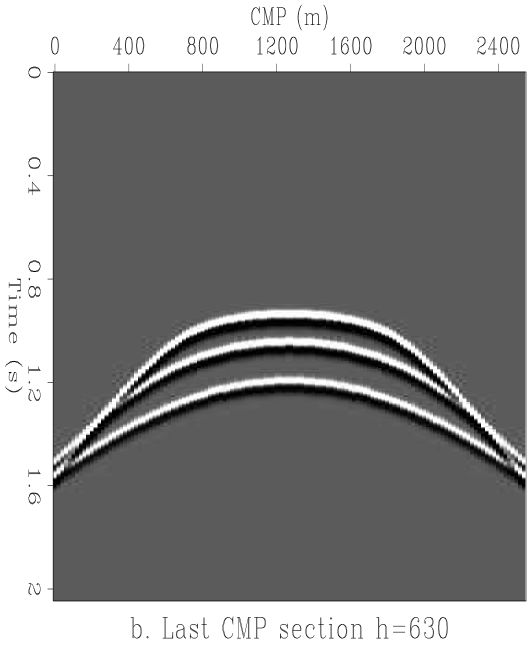

Figure 4: Constant-offset sections.
a. First constant-offset section, $h = 0m$.
b. Last constant-offset section, $h = 630m$. mihai-Fig4 [CR]

CONCLUSIONS

The straightforward implementation of the DSR equation uses constant samples of the variable k_h. This implementation introduces artifacts, erroneously attributed to Fourier wraparound in offset domain. By varying the sampling interval for k_h I eliminate these artifacts. This leads to a phase-shift prestack migration algorithm which can be applied to each offset separately. While this algorithm is slower overall compared to the classic DSR migration, it allows the migration of separate constant-offset sections which can be used for velocity analysis, amplitude versus offset studies and migration to zero-offset operator studies.

REFERENCES

Claerbout, J. C., 1985, Imaging the Earth's Interior: Blackwell Scientific Publications.

Popovici, A. M., 1993, Partial differential equation for migration to zero-offset: SEP–**77**, 77–90.

Yilmaz, O.,1979, Prestack partial migration: Ph.D. thesis, Stanford University.

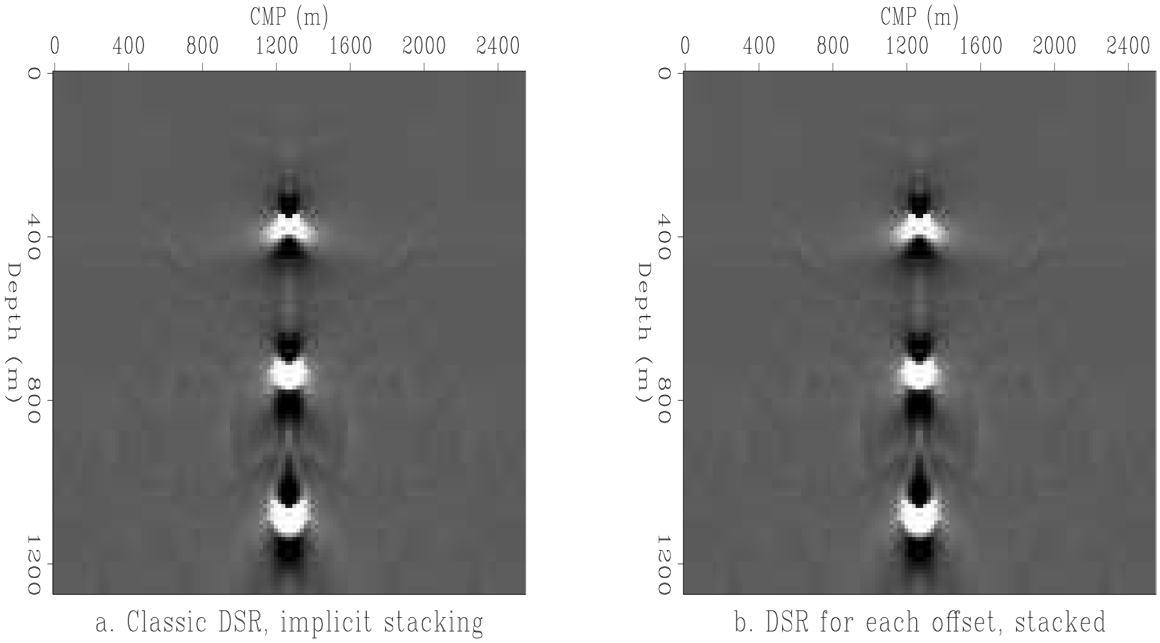

Figure 5: Migration of the whole prestack cube, using implicit stacking during downward continuation and stacking of the independently migrated constant-offset sections. **The two DSR algorithms produce identical results.**
a. Classic DSR in ω, k_y, k_h.
b. DSR for individual constant-offset sections, stacked. mihai-Fig5 [CR]

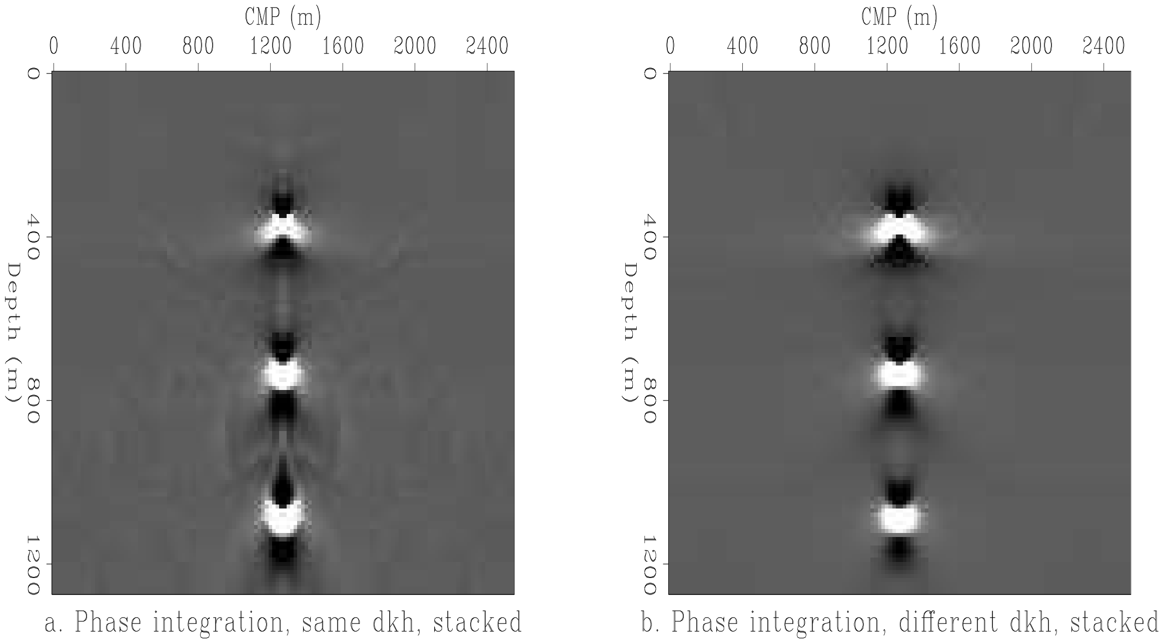

Figure 6: Comparison of constant-offset migration using constant k_h sampling and separate k_h spacings. Stacking greatly attenuates the artifacts in the constant-offset sections.
a. Constant sampling in k_h, stacked offsets.
b. Separate sampling in k_h, stacked offsets. $\boxed{\text{mihai-Fig6}}$ [CR]

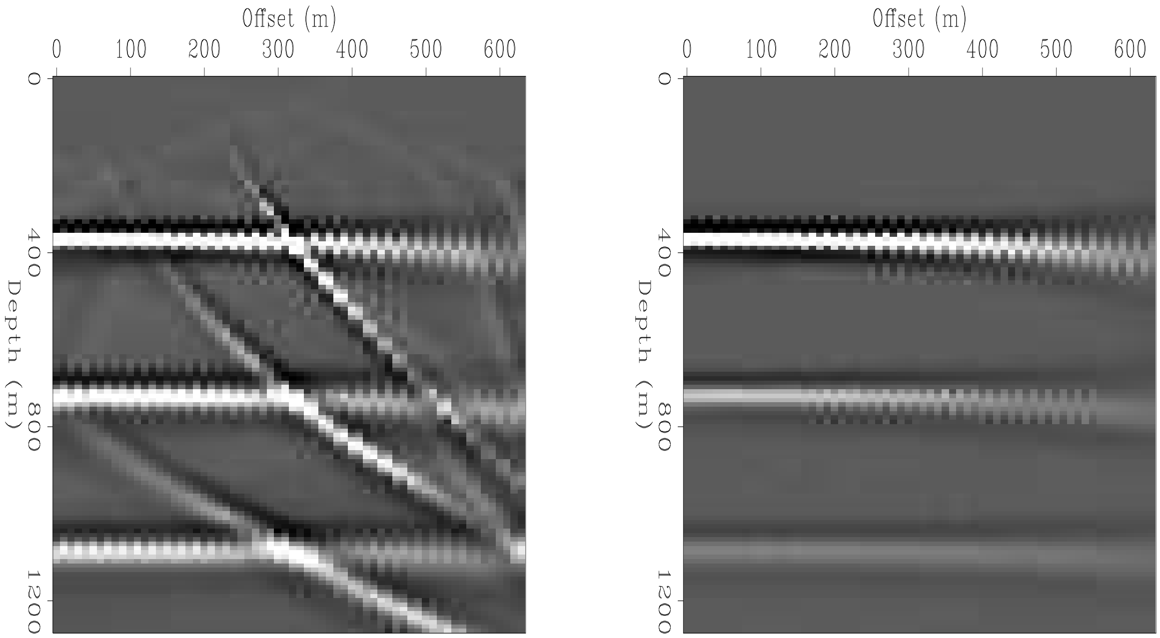

a. CMP section after DSR, same dkh

b. CMP section, different dkh

Figure 7: Common midpoint section, slicing vertically the three diffraction events. The artifacts in the DSR migration using constant k_h sampling are nonexistent in the DSR migration using separate sampling in k_h for each ω, k_y pair.
a. Constant sampling in k_h, stacked offsets.
b. Separate sampling in k_h, stacked offsets. $\boxed{\text{mihai-Fig7}}$ [CR]

Zauderer, E., 1989, Partial Differential Equations of Applied Mathematics: Wiley-Interscience.

APPENDIX A

Stationary phase approximation

Downward continuation using the DSR equation for a separate constant-offset sections requires the computation of the integral in equation (A-1). This can be done for all offsets by taking the inverse transform of the downward continuation exponential, or for a single offset by finding a stationary phase approximation to the integral

$$I = \int dk_h \; e^{ik_z(\omega,k_y,k_h)z - ik_h h}. \tag{A-1}$$

Integrals of the form

$$I(k) = \int_{-\infty}^{\infty} e^{ik\phi(t)} f(t) \; dt$$

are approximated asymptotically (Zauderer, 1989) when $k \to \infty$ by

$$I(k) \approx e^{ik\phi(t_0)} f(t_0) e^{\mathrm{sign}(\phi''(t_0))\frac{i\pi}{4}} \left[\frac{2\pi}{k \mid \phi''(t_0) \mid} \right]^{\frac{1}{2}}$$

where t_0 is the "stationary point" where the derivative of the phase is zero. The approximation described here assumes the second derivative is non-zero, which I will prove is the situation in this case.

The phase of the exponential in this case is

$$\phi(k_h) = -\mathrm{sign}(\omega) z \left[\sqrt{\frac{\omega^2}{v^2} - \frac{1}{4}(k_y + k_h)^2} + \sqrt{\frac{\omega^2}{v^2} - \frac{1}{4}(k_y - k_h)^2} \right] - k_h h. \tag{A-2}$$

In order to evaluate the stationary point we need to find the roots of the equation

$$\phi'(k_h) = -h + \mathrm{sign}(\omega) z \left[\frac{k_h + k_y}{\sqrt{\frac{\omega^2}{v^2} - \frac{1}{4}(k_y + k_h)^2}} + \frac{k_h - k_y}{\sqrt{\frac{\omega^2}{v^2} - \frac{1}{4}(k_y - k_h)^2}} \right]. \tag{A-3}$$

I was not able to find these roots, as it involves an equation of sixth degree. However, I will point out some properties of the phase, which should make the numerical computation simpler than the full integration.

The second derivative of the phase is non-zero, as it consists of the sum of four positive terms multiplied by sign(ω):

$$\phi''(k_h) = \frac{\mathrm{sign}(\omega)}{4}\left[\frac{1}{\sqrt{\frac{\omega^2}{v^2}-\frac{1}{4}(k_y-k_h)^2}} + \frac{(k_h-k_y)^2}{4\left[\frac{\omega^2}{v^2}-\frac{1}{4}(k_y-k_h)^2\right]^{\frac{3}{2}}} + \right. \tag{A-4}$$
$$\left. + \frac{1}{\sqrt{\frac{\omega^2}{v^2}-\frac{1}{4}(k_y+k_h)^2}} + \frac{(k_h+k_y)^2}{4\left[\frac{\omega^2}{v^2}-\frac{1}{4}(k_y+k_h)^2\right]^{\frac{3}{2}}}\right].$$

This ensures that there is no change in curvature, and the phase always has a maximum or a minimum and therefore a stationary point. Indeed, for a fixed pair of values ω, k_y, Figure A-1 shows the phase function for several depth levels. The sign of ω determines if the phase is positive or negative.

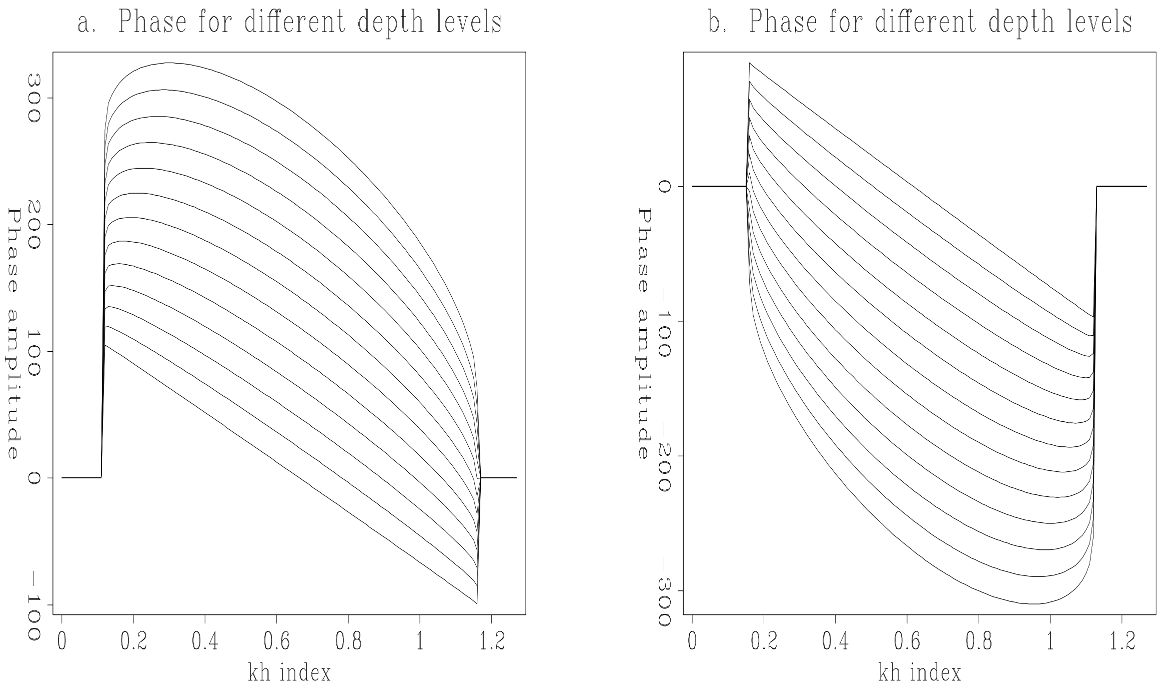

Figure A-1: Plot of the phase function for a constant pair of values ω, k_y. The different plots correspond to increasing depth levels.
a. Phase corresponding to positive ω.
b. Phase corresponding to negative ω. mihai-App1 [CR]